Key Engineering Materials
ISSN: 1662-9795, Vol. 774, pp 373-378
doi:10.4028/www.scientific.net/KEM.774.373

Online: 2018-08-01

Mixed-Mode Stress Intensity Factors for Tubes under Pure Torsion Loading

Jorge Guillermo Díaz Rodríguez[1,a], Luiz Fernando Nazaré Marques[2,b], Rolando Enrique Guzmán[3,c]

[1]Universidad Santo Tomás, facultad de Ingeniería Mecatronica. Carrera 18#9-27, Bucaramanga. Colombia

[2]Universidade Federal do Sul e Sudeste do Pará, UNIFESSPA. Av. dos Ipês s/n, barroio Nova Marabá, Marabá PA, 68500-000, Brasil

[3]Facultad de Ingeniería Mecánica, Universidad Pontificia Bolivariana, Campus Universitario Autopista Piedecuesta Km. 7, Bucaramanga, Colombia

[a]jorgeguillermo12@ustabuca.edu.co, [b]lfernando@unifesspa.edu.br, [c]rolando.guzman@upb.edu.co

Keywords: Stress Intensity factors, pure torsion, FEM, CTOD, CTSD

Abstract. Although it seems like a common load-geometry configuration, there is neither an analytical nor a numerical solution for Stress Intensity Factors (SIF) in cracked tubes under pure torsion. Standards such as API 579, BS 7910 or handbooks do not present such case. There is plenty of solutions based on FEM or weight functions calculations for an extensive load-geometry combinations, but not for tubes under pure torsion. This paper shows curves of K_I, K_{II}, and K_{III} for through-wall cracks obtained with ANSYS simulations for slim tubes, under pure torsion with a rounded horizontal slit, numerically calculated via J-integral. Additionally K_I, K_{II}, and K_{III} are calculated using relative displacement between two points along the crack lips using Linear Elastic Fracture Mechanics (LEFM) formulations for Crack Tip Opening Displacement (COD) and Crack Tip Sliding Displacement (CTSD). Results are compared with experimentally measured SIF using the Digital Image Correlation (DIC) technique for fatigued-growth cracks reported in literature.

Introduction

From already published results and posterior search in Stress Intensity Factors (SIF) manuals [1]–[4]or standards such as API, BS 7910, it was concluded that there is not available solution for thin tubes under pure torsion. Yang [5] published a numerical simulation results for rounded bars but the samples had a curvature perpendicular to the loading axis. Harter [6] published preliminary results for plates under biaxial loading, which is not the same case as here, but a tube can be approximated to a plate is the distances are sufficiently small and a biaxial loading case with equal stresses produces similar effects as torsion in an inclined crack. Hos [7] subjected slim tubes to remote pure torsion and Vormwald et. al. [8] reported measured SIF using the Digital Image Correlation (DIC) technique for fatigued-growth cracks using the same specimen. Because the reported SIF [8] came from experimental measurements, they already account for non-linear phenomena such as crack closure induced by plasticity, roughness, and environmental conditions. Therefore, they do not represent crack behavior under ideal linear elastic conditions. This paper deals with the numerical calculation for SIF in slim tubes subjected to pure torsion. Fig. 1 shows the schematics of the sample used, and the position of the four symmetrical cracks that were formed.

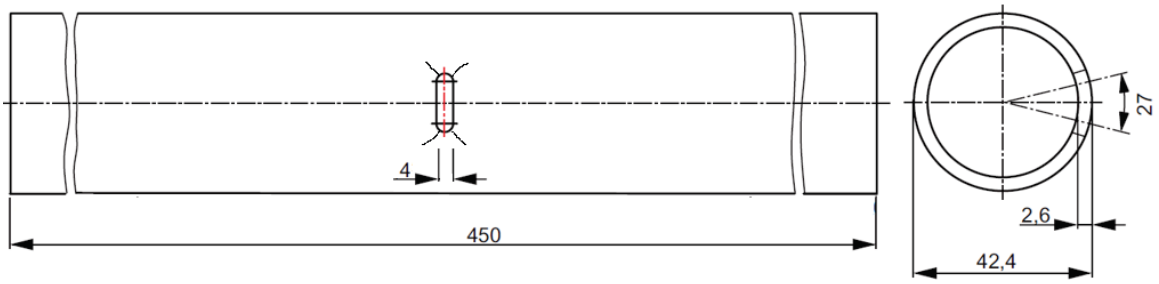

Fig. 1 Sample dimensions and generated cracks

Assuming local conditions do not cause large plasticity, the displacements for a flat cracked sample are described by Williams´s series [9] as presented in Eq. (1).

$$u=\sum_{n=1}^{\infty}\frac{r^{n/2}}{2G}\left(a_n\left\{\left[k+\frac{n}{2}+(-1)^n\right]C\mathrm{os}\frac{n\theta}{2}-\frac{n}{2}C\mathrm{os}\left(\frac{n-4}{2}\right)\theta\right\}-b_n\left\{\left[k+\frac{n}{2}-(-1)^n\right]Sin\frac{n\theta}{2}-\frac{n}{2}Sin\left(\frac{n-4}{2}\right)\theta\right\}\right).$$
$$\mathrm{v}=\sum_{n=1}^{\infty}\frac{r^{n/2}}{2G}\left(a_n\left\{\left[k-\frac{n}{2}+(-1)^n\right]Sin\frac{n\theta}{2}+\frac{n}{2}Sin\left(\frac{n-4}{2}\right)\theta\right\}+b_n\left\{\left[k-\frac{n}{2}+(-1)^n\right]Cos\frac{n\theta}{2}+\frac{n}{2}Cos\left(\frac{n-4}{2}\right)\theta\right\}\right). \quad (1)$$
$$w=\sum_{n=1}^{\infty}\left\{\frac{2r^{n-\frac{1}{2}}}{G}c_nSin\left(n-\frac{1}{2}\right)\theta\right\}.$$

where u, v and w are paralell, perpendicular to crack and out-of-plane displacements, respectively, G is shear modulus, k is the Kolosov constant, r and θ are coordinates respect a coordinate system with origin at the crack tip, n is the number of terms in the expansion series, a_1= $K_I/\sqrt{2\pi}$, b_1=$K_{II}/\sqrt{2\pi}$, c_1=$K_{III}/\sqrt{2\pi}$, and a_2=$\sigma_{ox}/4$, the so called T-stress.

If one takes two opposite-to-crack points along the crack faces and uses only the first term in the series presented in Eq. (1), SIF can be reduced to the expressions presented in Eq. (2). Herein, it is termed FEM COD method.

$$K_{I,II}=\frac{E\cdot COD_{I,II}}{4}\sqrt{\frac{2\pi}{r}}\quad;\quad K_{III}=\frac{E\cdot COD_{III}}{4(1+\nu)}\sqrt{\frac{2\pi}{r}}\quad. \quad (2)$$
$$COD_{\mathrm{I}}=v_A^{'}-v_B^{'}\qquad COD_{\mathrm{II}}=u_A^{'}-u_B^{'}\qquad COD_{\mathrm{III}}=w_A^{'}-w_B^{'}.$$

Now, if the applied load causes large plasticity around the crack tip, the ⌡ integral [10] can be used as crack driving force. It is presented in Eq. (3).

$$J=\int_{\Gamma}\left[W-\bar{\mathrm{T}}_i\frac{\delta u_i}{\delta x_i}\right]\delta s;\ (i=x,y). \quad (3)$$

where W is the strain energy density, u_i is displacement, x the crack growth direction, T is stress vector, and δs is length increment along an arbitrary chosen path. ⌡ is path independent for an open path. If more than one loading mode is present, ⌡ represents the sum of energy per unit area (J/m^2) in each loading direction. So, an orthogonal decomposition must be done to find the crack growth energy contribution on each axis, such as: ⌡ = ⌡$_{\mathrm{I}}$+ ⌡$_{\mathrm{II}}$+ ⌡$_{\mathrm{III}}$. One way to do so is by taking advantage of the displacements fields symmetry respect to the crack axis [11]. Another one way to decompose the ⌡ value found in numerical simulations is by using an auxiliary and already-known solution; a procedure identified as the M-integral [12]–[14]. Furthermore, if a contour is selected appropriately in the K-dominance zone, the elastic relation between ⌡ and SIF, as shown in Eq. (4) can be used.

$$J_i=\frac{K_i}{E'^2};i=I,II,III. \quad (4)$$

where E' is the elastic modulus depending on having a plane stress or a plane strain situation. ANSYS® uses the ⌡ formulation to calculate SIF through Eq. (4) using the displacements calculated in the numerical solution. Herein, it is termed FEM method

Materials and Methods

Modeling a meshing such a particular geometry is bit of a challenge. Two independent simulations were performed. In the first, a CAD model was created in Solidworks® and a simulation was ran in Solidworks Simulation® assuming the crack as a 0,1° sharp notch. The second simulation was done using the ANSYS® ADPL language. In both simulations, each model was meshed, and boundary conditions were applied to reproduce the specimen testing circumstances. The sample was meshed using 2mm SOLID186 in the general body. A 3mm radius refinement around the crack was done using 0,25mm quarter point elements in the ANSYS model, whereas in the SolidWorks® there were just refined tetrahedral elements. An example of the ANSYS® mesh is shown in Fig. 2. The applied load was 532N-m on the sample´s top face and a rigid support allocated in the lower face. Material properties were set to: elasticity modulus of 200GPa and Poisson ratio of 0,29. In neither case, no symmetry was used. There were ran simulations using different crack lengths, as presented ahead.

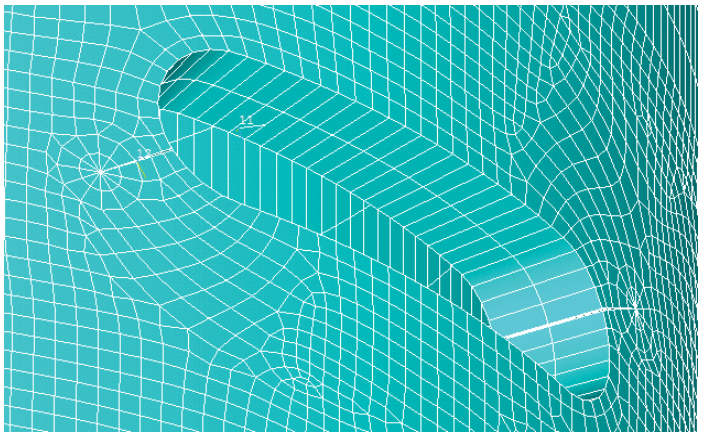

Fig. 2 ANSYS ® mesh details at cracks

For the Solidworks® model, displacements *u*, *v* and *w* along both crack lips were extracted and SIF in modes I, II, and III were calculated using Eq. (2). An example of opposite-to-crack points with respect to the known crack tip location is presented in Fig 3 where the Solidworks® mesh is also seen. On the other hand, for the ANSYS® model, the software already gives the SIF values.

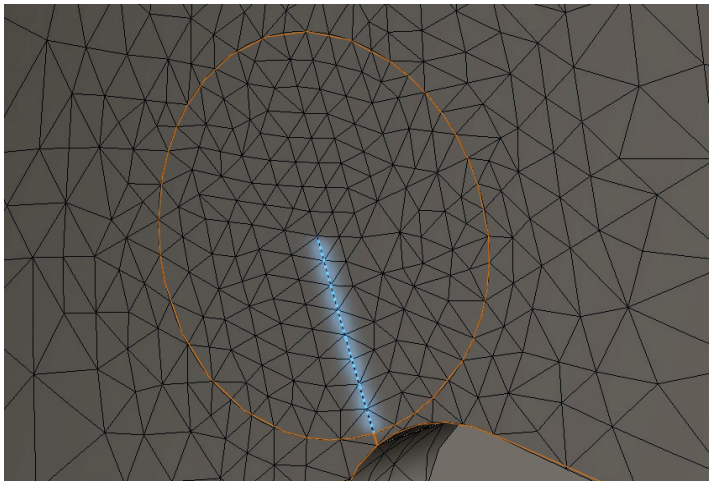

Fig. 3 Close up of SolidWorks® mesh around one crack

A job to obtain compliance functions is underway so a more general case, different load and thickness, could be addressed.

Results and Discussion

The published experimental results [8] were obtained with the DIC technique, so they are over-the-surface measurements. Fig. 4 shows the comparison maximum SIF mode I (over the surface) versus crack length. Because the short crack lengths, one cannot see clearly the proportionality to $1/\sqrt{r}$ predicted by theoretical models, for both numerical simulations, using Eq. 2 (FEM COD) and ANSYS (FEM) results.

As hinted before, the experimentally obtained SIF values, obtained with the DIC technique, account for plasticity and crack roughness. Additionally, the reported DIC values [8] represent a SIF range (ΔK), rather than an absolute value. This is due to an inherent characteristic of the technique, which needs a reference picture to establish displacements from.

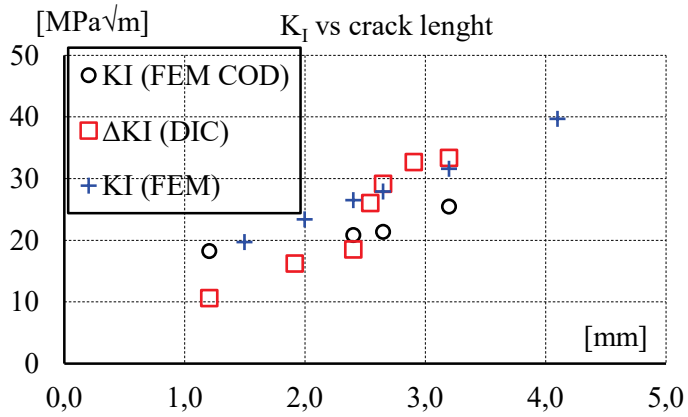

Fig. 4 SIF in mode I comparison with crack length

Fig. 5 shows the comparison maximum SIF mode II (over the surface) versus crack length.

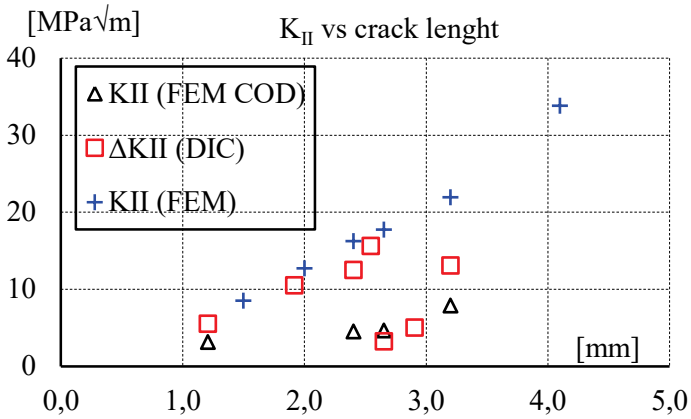

Fig. 5 SIF in mode II comparison with crack length

Finally, Fig. 6 shows the comparison maximum SIF mode II, also measured over the surface, versus crack length.

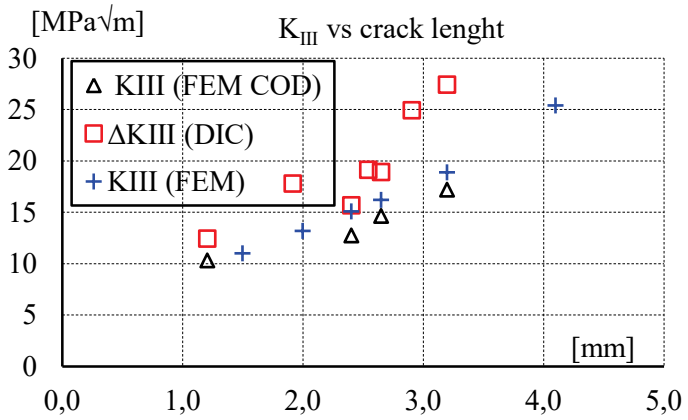

Fig. 6 SIF in mode III comparison with crack length

It is seen how although only in-plane loading was applied, out-plane sliding was present as well, which is represented by the K_{III} values, as described by the *w*-field in Eq. (1), and they are shown in Fig. 6.

Finally Fig. 7 shows how SIFs, calculated from Eq. 2 (COD method), develop according to distance from the crack tip. For K_I, the variation is negligible, as it stays almost constant as one moves away from the crack tip. For K_{II} and K_{III}, it is seen a variation with crack tip distance. Kibey, Sehitoglu, and Pecknold. [15] concluded that a crack may partially slip under mode II sliding when friction is included in the modeling. An analogy to mode III sliding can be drawn as well. In this case, the contact between faces was "frictionless", so a similar behavior cannot be assumed. The explanation for this must come from the uneven meshing around the two crack faces. Displacements in opposite-to-crack nodes do have the same distance to the CTL, therefore the $1/\sqrt{r}$ value in Eq. (3) has different values for the relative displacement between two almost-opposite-to-crack nodes.

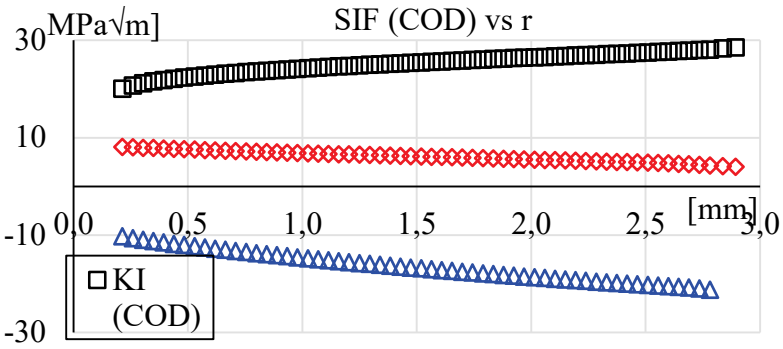

Fig. 7 Exemplary results of SIF versus crack tip distance

Conclusion

A simple method to calculate SIF using displacements from two opposite-to-crack points assuming linear elastic conditions was presented. The displacements were taken from FEM simulations that did not include special fracture mechanics special elements. The advantage of getting the SIF with this method is that it uses a simple solution and no specialized FEM software is needed.

Although the applied load was only in plane-loading (pure torsion), there were present mode I and mode III SIFs as well. This is due to the sample´s geometry and local conditions which allow out-of-plane displacements hence, generating large COD-z displacement values, thus associated K_{III} values. There were differences with experimental data reported in literature. This is attributed to non-linearities such as plasticity ahead of the plastic zone, and roughness between the crack faces that could hinder SIF mode II development.

References

[1] H. Tada, P. Paris, and G. Irwing, *The Stress Analysis of Cracks Handbook*. ASME, 2000.
[2] Y. Murakami, *Stress Intensity Factor Handbook*. New York: Pergamon Press, 1986.
[3] A. Prior, D. Rooke, and D. Cartwright, *Compendium of Stress Intensity Factors*. London: UK, Ministry of Defence, 1985.
[4] S. Laham and R. Ainsworth, *Stress Intensity Factor and Limit Load Handbook*. Brithish Energy, 1998.
[5] Y. Yang, "Linear elastic fracture mechanics-based simulation of fatigue crack growth under non- proportional mixed-mode loading," Technischen Universität Darmstadt, 2014.
[6] J. Harter, "K-Solutions for Through Cracks Under Biaxial Loading," in *AFGROW Workshop 2016*, 2016.
[7] Y. Hos, "Numerical and experimental investigation of crack growth in thin-walled metallic structures under nonproportional combined loading," Technischen Universität Darmstadt, 2017.
[8] M. Vormwald, Y. Hos, J. J. . Freire, G. L. . Gonzáles, and Diaz, "Crack tip displacement fields measured by digital image correlation for evaluating variable mode-mixity during fatigue crack growth," *Int. J. Fatigue*, vol. 113, 2018.
[9] M. L. Williams, "On the Stress State at the Base of a Stationary Crack," *J. Appl. Mech.*, vol. 24, no. march, pp. 109–114, 1957.
[10] J. R. Rice, "A Path Independent Integral and the Approximate Analysis of Strain Concentration by Notches and Cracks," *J. Appl. Mech.*, vol. 35, no. 2, pp. 379–386, 1968.
[11] M. R. Molteno and T. H. Becker, "Mode I – III Decomposition of the J -integral from DIC Displacement Data," *Strain*, vol. 51, no. 6, pp. 492–503, 2015.
[12] J. F. Yau, S. S. Wang, and H. T. Corten, "A Mixed-Mode Crack Analysis of Isotropic Solids Using Conservation Laws of Elasticity," *J. Appl. Mech.*, vol. 47, no. 2, p. 335, 1980.
[13] M. Gosz and B. Moran, "An interaction energy integral method for computation of mixed-mode stress intensity factors along non-planar crack fronts in three dimensions," *Eng. Fract. Mech.*, vol. 69, no. 3, pp. 299–319, 2002.
[14] P. A. Wawrzynek, B. J. Carter, and L. Banks-Sills, "The M-integral for computing stress intensity factors in generally anisotropic materials," 2005.
[15] S. Kibey, H. Sehitoglu, and D. A. Pecknold, "Modeling of fatigue crack closure in inclined and deflected cracks," *Int. J. Fatigue*, vol. 129, no. 3, pp. 279–308, 2004.